Whole-Genome Sequencing Identifies Genetic Variances in Culture-Expanded Human Mesenchymal Stem Cells

Jun Cai,[1] Xuexia Miao,[1,2] Yueying Li,[1] Cory Smith,[3,4] Kitman Tsang,[4] Linzhao Cheng,[3,4,*] and Qian-fei Wang[1,*]

[1]Laboratory of Genome Variations and Precision Bio-Medicine, Beijing Institute of Genomics, Chinese Academy of Sciences, Beijing 100101, China
[2]University of Chinese Academy of Sciences, Beijing 100049, China
[3]Predoctoral Training Program in Human Genetics, Johns Hopkins University School of Medicine, Baltimore, MD 21205, USA
[4]Stem Cell Program, Institute for Cell Engineering, and Division of Hematology, Johns Hopkins University School of Medicine, Baltimore, MD 21205, USA
*Correspondence: lcheng2@jhmi.edu (L.C.), wangqf@big.ac.cn (Q.-f.W.)
http://dx.doi.org/10.1016/j.stemcr.2014.05.019
This is an open access article under the CC BY-NC-ND license (http://creativecommons.org/licenses/by-nc-nd/3.0/).

SUMMARY

Culture-expanded human mesenchymal stem cells (MSCs) are increasingly used in clinics, yet full characterization of the genomic compositions of these cells is lacking. We present a whole-genome investigation on the genetic dynamics of cultured MSCs under ex vivo establishment (passage 1 [p1]) and serial expansion (p8 and p13). We detected no significant changes in copy-number alterations (CNAs) and low levels of single-nucleotide changes (SNCs) until p8. Strikingly, a significant number (677) of SNCs were found in p13 MSCs. Using a sensitive Droplet Digital PCR assay, we tested the nonsynonymous SNCs detected by whole-genome sequencing and found that they were preexisting low-frequency mutations in uncultured mononuclear cells ($\sim$0.01%) and early-passage MSCs (0.1%–1% at p1 and p8) but reached 17%–36% in p13. Our data demonstrate that human MSCs maintain a stable genomic composition in the early stages of ex vivo culture but are subject to clonal growth upon extended expansion.

INTRODUCTION

Human mesenchymal stem cells (MSCs) are multipotent cells that show potential to differentiate into cells of diverse lineages such as bone, cartilage, fat, and tendon (Prockop, 1997). MSCs have been used in cell-based therapies for treating bone and cardiovascular defects and a variety of other degenerative diseases and tissue injuries, representing a fast-growing field in regenerative medicine (Salem and Thiemermann, 2010; Wang et al., 2012; Bianco et al., 2013). MSCs also confer beneficial effects in the modulation of immune and inflammatory responses and are used in various clinical trials for treating graft-versus-host disease and other immune diseases (DelaRosa et al., 2012).

Although MSCs can be isolated from different adult tissues such as marrow and adipose, native MSCs are rare (1 per 10,000–100,000 mononuclear cells [MNCs]) in marrow and other adult tissues (Prockop, 1997). Thus, ex vivo expansion of MSCs by serial cell culture and passages (lasting for months) is required to reach an effective cell dose for one or multiple recipients. Although MSC-based therapies have achieved some success and appeared safe in the early stages of clinical follow-up (Salem and Thiemermann, 2010; Wang et al., 2012; DelaRosa et al., 2012), a full characterization of these vastly expanded cells in serial cultures is lacking.
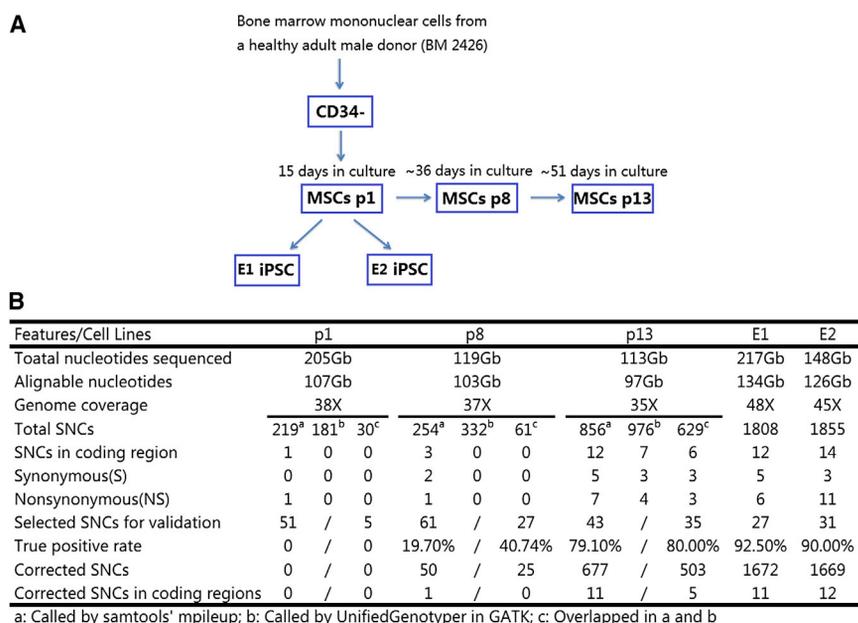
Maintenance of stem cell genome integrity is thought to be crucial to their safe implementation in clinical therapies. While induced pluripotent stem cells (iPSCs) have been extensively studied by various methods including whole-genome sequencing (WGS; Cheng et al., 2012; Gore et al., 2011; Young et al., 2012; Hussein et al., 2011), MSCs have not been evaluated to a similar extent despite their longer history and wide clinical use. The analyses from Ben-David et al. suggested the acquisition of chromosomal aberrations in human adult MSCs as well as neural stem cells (Ben-David et al., 2011), although they could not compare these cells directly with the seeding primary cells. However, Sensebe et al. argued that chromosomal aberrations are rather limited in human adult MSCs, based on a review of existing data in current literature (Ferreira et al., 2012; Sensebé et al., 2012). In Han et al.'s recent study, human umbilical cord mesenchymal stem cells (MSCs) exhibited copy-number alterations (CNAs) after extended long-term culture at passage 30 (Wang et al., 2013). Therefore, the genome integrity of clinic-used MSCs (5–13 passages) is still largely unexplored at the genome-wide level except for a few reports, most of which were based on low-resolution technologies (Prockop and Keating, 2012). In this study, we investigated the rate and level of genetic alterations in MSCs along serial culture passages after derivation from adult marrow MNCs.

RESULTS

Characterization of Culture-Expanded MSCs

To investigate whole-genome dynamic changes during the ex vivo establishment and expansion of human MSCs, we

A

Bone marrow mononuclear cells from
a healthy adult male donor (BM 2426)

↓

CD34-

↓ 15 days in culture → ~36 days in culture → ~51 days in culture

MSCs p1 → MSCs p8 → MSCs p13

↓

E1 iPSC   E2 iPSC

B

Features/Cell Lines	p1			p8			p13			E1	E2
Toatal nucleotides sequenced	205Gb			119Gb			113Gb			217Gb	148Gb
Alignable nucleotides	107Gb			103Gb			97Gb			134Gb	126Gb
Genome coverage	38X			37X			35X			48X	45X
Total SNCs	219[a]	181[b]	30[c]	254[a]	332[b]	61[c]	856[a]	976[b]	629[c]	1808	1855
SNCs in coding region	1	0	0	3	0	0	12	7	6	12	14
Synonymous(S)	0	0	0	2	0	0	5	3	3	5	3
Nonsynonymous(NS)	1	0	0	1	0	0	7	4	3	6	11
Selected SNCs for validation	51	/	5	61	/	27	43	/	35	27	31
True positive rate	0	/	0	19.70%	/	40.74%	79.10%	/	80.00%	92.50%	90.00%
Corrected SNCs	0	/	0	50	/	25	677	/	503	1672	1669
Corrected SNCs in coding regions	0	/	0	1	/	0	11	/	5	11	12

a: Called by samtools' mpileup; b: Called by UnifiedGenotyper in GATK; c: Overlapped in a and b

Figure 1. Culture and Whole-Genome Sequencing of Adult Marrow MSCs and Derived iPSC Lines
(A) Relationship of adult bone marrow cells, MSCs at various passages, and derived MSCs from the same healthy male donor. After depleting CD34$^+$ hematopoietic progenitor cells, CD34$^-$ marrow MNCs were used to establish adherent MSCs culture or used for sequencing analyses. The early MSC culture (p1) was used to either derive iPSC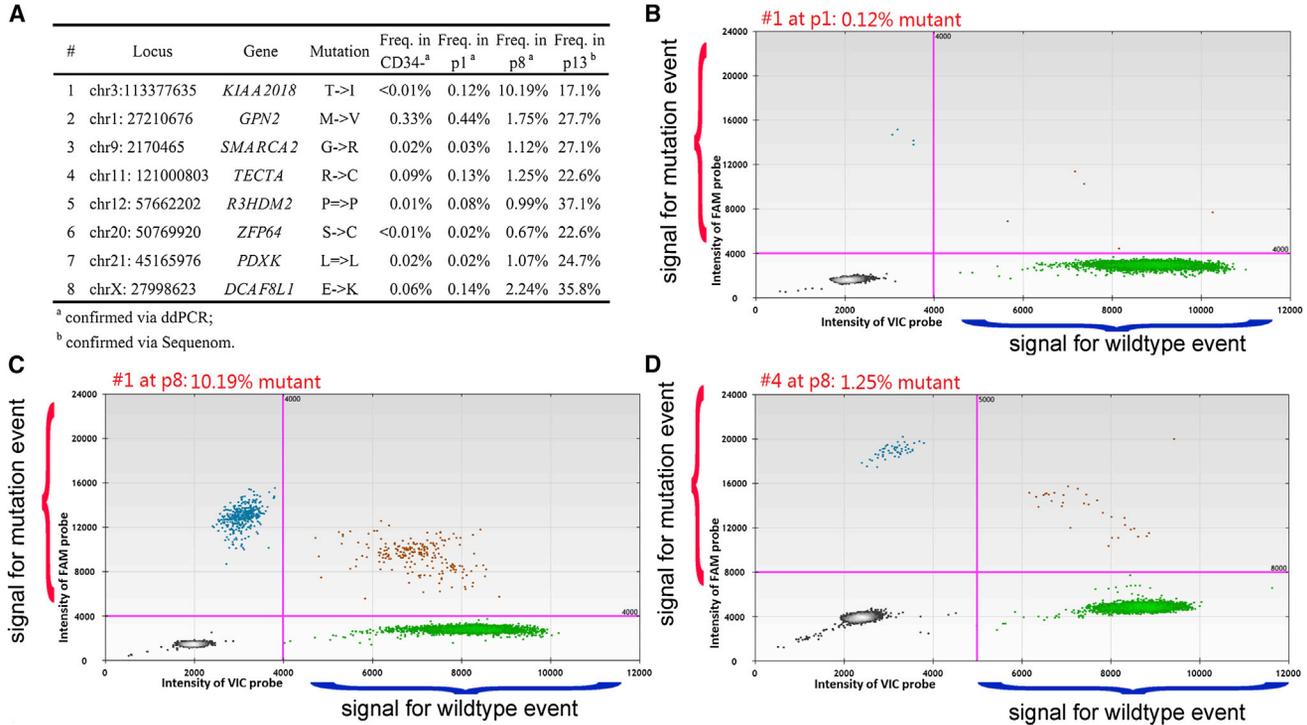 lines (E1 and E2) or further expand MSCs until p13. (B) Summary of the whole-genome sequencing data and the comparison of SNCs among cultured MSCs and iPSCs. The raw sequencing data of cell line E1 was derived from the parental study, and the numbers of SNCs for E1 were cited from a previous paper (Cheng et al., 2012).

used bone marrow MNCs from a healthy 31-year-old male donor. The CD34$^+$ hematopoietic progenitor cells from the same donor have been previously used (after 4-day culture) to derive iPSC lines that were fully sequenced (Cheng et al., 2012). The CD34-delepted (CD34$^-$) cells (>97% of the total marrow MNCs) were used to establish a MSC population that adheres to tissue culture plastic and proliferates rapidly. The established MSCs (passage 1 [p1], 15 days in culture) were either used to generate two iPSC lines (E1 and E2) or further expanded for an additional 36 days (a total of 51 days) until p13 (Figure 1A). The MSCs were characterized by standard methods including morphology and cell-surface protein profiles as we previously reported (Cheng et al., 2003; Zou et al., 2012). The culture-expanded MSC population (p1) shows a typical morphology and expresses cell-surface markers such as CD29, CD73, CD90 (Thy-1) and CD105 but lacks CD14, CD34, or CD45. After p1, MSCs can rapidly expand as undifferentiated cells in the seven subsequent passages, with approximately three cell-population doublings per passage every 3 days until p8. After p8, MSC proliferation slows down but cells could expand with an additional 12 cell-population doublings until p13. The later-passage cells (p10–p13) showed increased cell size and decreased nucleus/plasma ratio. The clonal efficiency of culture-expanded MSCs varies: ~20% of p1 to p8 MSCs will form sizable colonies (after 10–14 days), while the clonal efficiency of p13 MSCs is <5%. However, MSCs tested at p5, p8, and p13 showed similar differentiation potential as p1 by the standard in vitro assays of MSC osteogenesis and adipogenesis.

Identification of Somatic Mutations in Late-Passage MSC Culture

We applied the HiSeq2000 WGS method to the uncultured CD34$^-$ cells, the initial establishment of MSCs (p1), culture-expanded p8 and p13 MSCs, and the iPSC line E2 derived from p1 MSCs (Figure 1A; E1 was sequenced previously; Cheng et al., 2012). We identified a small number of single-nucleotide changes (SNCs) in the earlier MSC cultures (p1, 219; p8, 254), while a significant number of somatic mutations (856) were found in p13 MSCs (Figure 1B).

Large-scale and massively parallel sequencing is not perfect and presents false-positive calls in SNC identification (Ajay et al., 2011). Thus, we used a mass spectrometry-based Sequenom assay to systematically validate the identified SNCs. One-fourth of the SNCs (51 out of 219) present in p1 were randomly selected, but all were confirmed to be false-positive calls. For the randomly selected 61 (out of 254) SNCs in p8, 12 were confirmed to be the true positives. We further selected all coding (12) and 31 (out of 844) non-coding SNCs identified in p13 for Sequenom validation and were able to confirm 91% (11/12) of coding and 74% (23/31) of noncoding SNCs. The validation result via Sequenom assay is summarized in Table S1 (available online) Based on the results obtained by Sequenom validation, the true-positive rates of SNCs in p1, p8, and p13 were estimated to be 0% (0/51), 19.7% (12/61), and 79.1% (34/43), respectively (Figure 1B; Table S1), from which we finally corrected the numbers of true SNCs in p1, p8, and p13 to be 0, 50, and 677, respectively (Figure 1B). These results suggest that few SNCs emerged in early-cultured MSCs until p8. Additionally, all genomes examined were diploid,

A

#	Locus	Gene	Mutation	Freq. in CD34-[a]	Freq. in p1[a]	Freq. in p8[a]	Freq. in p13[b]
1	chr3:113377635	KIAA 2018	T->I	<0.01%	0.12%	10.19%	17.1%
2	chr1: 27210676	GPN2	M->V	0.33%	0.44%	1.75%	27.7%
3	chr9: 2170465	SMARCA2	G->R	0.02%	0.03%	1.12%	27.1%
4	chr11: 121000803	TECTA	R->C	0.09%	0.13%	1.25%	22.6%
5	chr12: 57662202	R3HDM2	P=>P	0.01%	0.08%	0.99%	37.1%
6	chr20: 50769920	ZFP64	S->C	<0.01%	0.02%	0.67%	22.6%
7	chr21: 45165976	PDXK	L=>L	0.02%	0.02%	1.07%	24.7%
8	chrX: 27998623	DCAF8L1	E->K	0.06%	0.14%	2.24%	35.8%

[a] confirmed via ddPCR;
[b] confirmed via Sequenom.

B

C

D

Figure 2. Detection of the Rare SNC by Droplet Digital PCR

(A) The confirmed frequencies of the coding SNCs in different stages of cells from in vivo (CD34⁻ cells) to ex vivo (p1, p8, and p13 MSCs). (B–D) Demonstration of frequency analysis by Droplet Digital PCR (ddPCR) for SNC #1 at p1 and p8 and #4 at p8. y axis: the signal intensities of FAM probe for the mutant allele; x axis: the signal intensities of VIC probe for the reference allele. Each scatter dot represents a PCR signal in a droplet. Counting of ddPCR signals for the mutation (red bar) and reference (blue bar) resulted in the frequency estimation of 0.12%, 10.19%, and 1.25%, respectively. The pink horizontal and vertical lines were automatically determined based on both cluster separation of the four-color dots and the calibration of nontemplate control in ddPCR experiments by the QX100 ddPCR system. The primers and probes designed for #1 and #4 were distinct, so the cutoff rule was unique for each SNC.

and no CNAs were detected significantly above WGS background over the course of 13 culture passages (Figure S1).

Somatic Changes Identified in Late Passages Were Preexisting Low-Frequency Mutations in the Uncultured Cell Population

As a significant number of somatic mutations were observed in the p13 culture, but not the p1 and p8 MSC culture, it is not clear whether the observed SNCs were pre-existing rare mutations of the original cell population or if they are newly occurring genetic mutations during culture expansion. To distinguish these two possibilities, we employed a sensitive Droplet Digital PCR assay (ddPCR), which permits quantitative detection of rare molecules and results in a reliable measurement of SNC frequencies as low as 0.01% (Hindson et al., 2011; Abyzov et al., 2012). Among all 11 Sequenom-confirmed coding SNCs identified in p13, the primers and probes of eight SNCs were successfully designed for ddPCR experiments. These eight SNCs were further examined for their frequencies in

primary CD34⁻ cells and different stages of MSCs (p1 and p8) using the ddPCR assay (Figure 2A; Table S2). The signals for precise estimation of the frequencies of 0.12% (#1 at p1), 10.19% (#1 at p8), and 1.25% (#4 at p8) via ddPCR are demonstrated in Figures 2B–2D. Strikingly, all of the eight SNCs were detected as low-frequency ones in uncultured CD34⁻ MNCs (0.01%–0.05%) and early-passage MSCs (0.01%–0.2% at p1) but rose to 0.63%–10.19% in p8 and 17%–36% in p13 MSCs (Figure 2A). Our data demonstrate that all the "new" point mutations present in the culture-expanded p8 or p13 MSCs preexisted in the early cell population, albeit at a very low frequency.

Identification of Somatic Mutations in Induced Pluripotent Stem Cell Lines Generated from the Same Donor

To compare the level of genetic variance observed in culture-expanded MSCs to that accumulated in iPSCs, we generated two independent iPSC lines (E1 and E2) from the initial establishment of MSCs (p1) of the same donor (Figure 1A).
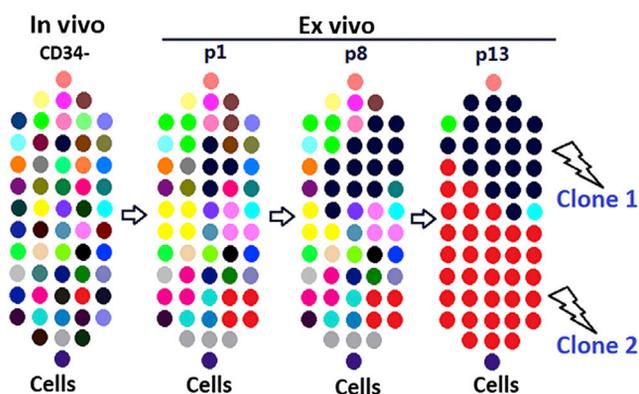
Figure 3. A Working Model of Clonal Expansion to Explain Observed SNCs in Culture-Expanded MSCs Derived from Adult Marrow Cells

Close circles of different colors represent cells with distinct single-nucleotide changes (SNCs). The number of circles for each color indicates the frequency of distinct SNCs in the mixed cell population. Cells derived from the same ancestor are marked with an identical color along serial ex vivo culture passages (p1, passage 1; p8, passage 8; and p13, passage 13). The emergence of multiple low-frequency SNCs in primary MNCs (uncultured CD34⁻ cells) indicates the existence of small clones that carry unique private somatic mutations. In addition, culture-expanded human MSCs maintain a relatively stable genomic composition in the early stages of ex vivo culture (p1). However, drastically increased frequencies of pre-existing mutations suggest dominant clonal growth of two independent MSC populations (clone 1 and clone 2) upon extended expansion in p8 and p13.

No CNAs were found in the two iPSC lines as in a previous analysis of the E1 iPSC line (Cheng et al., 2012). Compared to the uncultured cells or p1 MSCs, each of the two iPSC lines harbored 1,672 specific SNCs (11 in the coding region) and 1,669 specific SNCs (12 in the coding region), based on a true-positive rate of ~90% (Figure 1B; Table S1).

Interestingly, identified genome-wide SNCs were not shared between the two iPSC lines or with SNCs found in other sequenced iPSC cell lines (Gore et al., 2011). Consistent with this result, studies show that mutations identified in human iPSCs do not facilitate the acquisition of pluripotency and do not provide a selective advantage for reprogramming (Young et al., 2012; Ruiz et al., 2013). However, the higher ratio of coding SNCs in MSCs (11/677, or 1.62%) compared to that in iPSCs (11/1672 or 0.65%) may reflect a higher rate of coding changes during the positive selection of specific cell clones in the MSC population.

DISCUSSION

Our report represents a genome-wide study to understand the genetic variance in culture-expanded human MSCs.

The emergence of multiple low-frequency SNCs in primary marrow MNCs (Figure 2A) indicates the existence of small clones carrying unique private somatic mutations, consistent with a recent report describing the mosaic genomic composition of normal human skin cell populations (Abyzov et al., 2012; Biesecker and Spinner, 2013). Two lines of evidence suggest that human culture-expanded MSCs maintain a relatively stable genomic composition in the early stages of ex vivo culture. The first is the lack of significant somatic mutations (SNCs and CNAs) as shown by WGS analyses. Second, the specific SNCs in coding regions had similarly low frequencies, ranging from 0.01% to 0.2% in both primary MNCs and p1 MSCs. However, a gradual rise in the frequencies of specific coding SNCs was observed from ~0.1% (p1 MSCs) to ~1% (p8 MSCs; Figures 2A and 3). Moreover, the frequencies of these rare mutations were dramatically increased during the culture leading to p13, suggesting dominant clonal growth of a specific MSC population upon extended expansion. Interestingly, close examination of the dynamic changes in the mutation frequencies revealed a pattern of two independently evolved subclonal populations (Figure 3). The first clone was characterized by a G-to-A SNC that resulted in a threonine (T) to isoleucine (I) amino acid change in the KIAA2018 gene (#1 in Figure 2A). The frequency of this SNC was kept between 0.01% and 1% before it reached 10% in p8 and 17% in p13 MSC, suggesting the occurrence of a dominative clonal population at p8. The remaining seven coding changes (#2–#8 in Figure 2A) were in low frequencies in p8 but achieved allele frequencies between 22% and 37% in p13, which was much higher than that for the #1 SNC (17%, defining the first clone). These data suggest that #2–#8 coding SNCs may define a separate cell population that only reaches dominance at p13 (Figure 3).

In p13 MSC culture, we detected the expansion of cells containing pre-existing missense SNCs in likely important genes such as *ZFP64*, *SMARCA2*, and *KIAA2018* (Figure 2A). *ZFP64* expresses in a broad range of mesenchymal tissues of mouse embryos and is detected in diverse mesenchymal cell lines. As a coactivator of *NOTCH1*, *ZFP64* has been shown to directly regulate myogenic and osteoblastic differentiation in mesenchymal cells (Sakamoto et al., 2008). *SMARCA2* is part of the SWI/SNF chromatin-remodeling complex that is essential for embryonic stem cells (ESCs) to maintain their normal proliferation and pluripotency (Yan et al., 2008). Proteomic analysis also demonstrates that *SMARCA2* interacts with key stem cell factor *KLF4* in pluripotent stem cells (Mak et al., 2010). Interestingly, the expression of *SMARCA2* is specifically upregulated in mesenchymal progenitors derived from human ESCs (Denis et al., 2011). Genetic polymorphism of *KIAA2018* was identified in genome-wide meta-analysis related to human bone

metabolism, an important mesenchymal stem cell-derived tissue (Estrada et al., 2012). In addition, genomic variants in *ZFP64* and *DCAF8L1* have been shown to be associated with various human cancers (Sjöblom et al., 2006; Park et al., 2013). More functional studies are required to assess if the observed nonsynonymous SNCs may provide a growth advantage upon extended ex vivo culture that leads to the outgrowth of specific MSCs that carry those mutations. It would also be interesting to see if MSCs that can be cultured for longer periods, like fetal tissue MSCs and human ESC-derived MSCs, also show an enrichment of these SNCs and if the presence of these SNCs is correlated with changes in gene expression.

Our findings have important implications for the safety evaluation of human MSC-based stem cell therapies. The number of passages of culture-expanded human MSCs that are used in more than 200 clinical trials is not always clear (Bianco, 2013). Although academic centers tend to use low-passage (likely less than five to eight passages) culture-expanded MSCs for their small-scale clinical trials, it is understandable that commercial identities would prefer to use massively expanded MSCs of few lots (and therefore higher passage numbers) to reduce the cost and regulatory requirements associated with the establishment of each lot. In this study, we provide direct evidence that there are no significant changes in CNAs and only low levels of SNCs by p8 using state-of-the-art WGS technology. However, culture-expanded MSCs at early passages still contain rare cells with missense SNCs that could be manifested ex vivo (as we observed in the p13 culture) or in vivo if a small fraction of MSCs were sustained and amplified after infusion. As our data were obtained from a small sample size of fully sequenced MSC genomes, further investigation is warranted to determine the clinical significance of these findings.

EXPERIMENTAL PROCEDURES

Sample Preparation
Human primary MNCs were obtained from the bone marrow of a healthy male donor aged 31 years. The practice of using human samples for laboratory research, including cell culture and iPSC derivation, was approved by the internal review board of Johns Hopkins University, where the cell cultures were conducted. The CD34-depleted (CD34−) MNCs purified with a magnetic-activating cell sorting magnet system were used to establish MSCs using a standard protocol (Cheng et al., 2012). MSCs are selectively expanded from primary cultures of bone marrow MNCs by their tendency to adhere to tissue culture plastic (Cheng et al., 2003; Zou et al., 2012).

Sequencing Data and Mutation Calling in MSCs and iPSCs
WGS libraries of all of the samples were constructed according to the manufacturers' standard protocols of Hiseq2000. A total

of 2 × 100 bp paired-end reads were produced using the Hiseq2000 system. The uniquely alignable reads on NCBI37/hg19 using the Burrows-Wheeler Alignment tool algorithm were retained for downstream analysis (Li and Durbin, 2009). Using the uncultured CD34− MNCs as a control, SNC candidates were collected by "mpileup" command line in SAMTools as well as UnifiedGenotyper in GATK (Li et al., 2009; DePristo et al., 2011). Quality recalibration and local realignment were performed in the GATK pipeline before variation calling. The following criteria were applied for mutations calling between pairwise samples: (1) variant sites had a minimum coverage of 20 and Phred-scaled base quality above 15; (2) the mutant allele frequency of SNCs in MSCs or iPSCs was above 0.2 or 0.3, respectively, whereas it was zero in the control sample; (3) the mutant allele was supported by at least two reads in the forward strand and two reads in the reverse strand; and (4) the sites in the dbSNP were excluded. We utilized breakpoints, read depths, and minor allele frequencies of heterozygous sites for detection of CNAs (Abyzov et al., 2011; Chen et al., 2009).

Genotyping Validation by Sequenom
The Sequenom platform was employed to verify the SNCs identified in MSCs and iPSCs (Bradić et al., 2011). The percentage of mutant allele was determined using the default settings of the MassARRAYTyper 4.0 Analyzer.

Digital PCR to Detect Precise Allele Frequencies of SNCs
Digital PCR was performed on the Bio-Rad QX100 ddPCR system (Hindson et al., 2011). Poisson statistics was applied to quantify the precise DNA of mutant alleles and estimate the frequency of each SNC based on counts of the positive and negative droplets. Both nontemplate controls containing TE buffer (10 mM Tris/0.1mM EDTA [pH 8.0]) and template controls with blood DNA from another healthy donor were used to eliminate low-level template contamination and systematic bias.

Examination of Clonal Composition of the Cell Population
The dynamic frequencies of the SNCs provided some clues about the composition of the cells. If and only if an SNC represents a moderate frequency in the cell population, a cell carrying this SNC has been expanded to be a dominating subclone lineage. So, there were some dominating subclones in p8 and p13 MSCs. If SNC A sequentially occurred in mutant cells with the preexisting SNC B, the frequency of SNC B would always be higher than that of SNC A, and vice versa. Thus, we deduced that the cells carrying SNC #1 formed a unique subclone lineage, whereas another separate cell clone that only reached dominancy at p13 was defined by the other seven SNCs in our case.

ACCESSION NUMBERS

AUTHOR CONTRIBUTIONS

L.C., Q.W., and J.C. designed the study. K.T. and L.C. provided samples. J.C., X.M., Q.W., and L.C. analyzed and interpreted the data. X.M. performed the sequencing and validation experiments. Y.L., C.S., and K.T. helped with the experiments and the data analysis. Q.W., L.C., and J.C. wrote the manuscript.

REFERENCES

Abyzov, A., Urban, A.E., Snyder, M., and Gerstein, M. (2011). CNVnator: an approach to discover, genotype, and characterize typical and atypical CNVs from family and population genome sequencing. Genome Res. *21*, 974–984.

Abyzov, A., Mariani, J., Palejev, D., Zhang, Y., Haney, M.S., Tomasini, L., Ferrandino, A.F., Rosenberg Belmaker, L.A., Szekely, A., Wilson, M., et al. (2012). Somatic copy number mosaicism in human skin revealed by induced pluripotent stem cells. Nature *492*, 438–442.

Ajay, S.S., Parker, S.C., Abaan, H.O., Fajardo, K.V., and Margulies, E.H. (2011). Accurate and comprehensive sequencing of personal genomes. Genome Res. *21*, 1498–1505.

Ben-David, U., Mayshar, Y., and Benvenisty, N. (2011). Large-scale analysis reveals acquisition of lineage-specific chromosomal aberrations in human adult stem cells. Cell Stem Cell *9*, 97–102.

Bianco, P. (2013). Don't market stem-cell products ahead of proof. Nature *499*, 255.

Bianco, P., Cao, X., Frenette, P.S., Mao, J.J., Robey, P.G., Simmons, P.J., and Wang, C.Y. (2013). The meaning, the sense and the significance: translating the science of mesenchymal stem cells into medicine. Nat. Med. *19*, 35–42.

Biesecker, L.G., and Spinner, N.B. (2013). A genomic view of mosaicism and human disease. Nat. Rev. Genet. *14*, 307–320.

Bradić, M., Costa, J., and Chelo, I.M. (2011). Genotyping with Sequenom. Methods Mol. Biol. *772*, 193–210.

Chen, K., Wallis, J.W., McLellan, M.D., Larson, D.E., Kalicki, J.M., Pohl, C.S., McGrath, S.D., Wendl, M.C., Zhang, Q., Locke, D.P., et al. (2009). BreakDancer: an algorithm for high-resolution mapping of genomic structural variation. Nat. Methods *6*, 677–681.

Cheng, L., Hammond, H., Ye, Z., Zhan, X., and Dravid, G. (2003). Human adult marrow cells support prolonged expansion of human embryonic stem cells in culture. Stem Cells *21*, 131–142.

Cheng, L., Hansen, N.F., Zhao, L., Du, Y., Zou, C., Donovan, F.X., Chou, B.K., Zhou, G., Li, S., Dowey, S.N., et al.; NISC Comparative Sequencing Program (2012). Low incidence of DNA sequence variation in human induced pluripotent stem cells generated by nonintegrating plasmid expression. Cell Stem Cell *10*, 337–344.

DelaRosa, O., Dalemans, W., and Lombardo, E. (2012). Mesenchymal stem cells as therapeutic agents of inflammatory and autoimmune diseases. Curr. Opin. Biotechnol. *23*, 978–983.

Denis, J.A., Rochon-Beaucourt, C., Champon, B., and Pietu, G. (2011). Global transcriptional profiling of neural and mesenchymal progenitors derived from human embryonic stem cells reveals alternative developmental signaling pathways. Stem Cells Dev. *20*, 1395–1409.

DePristo, M.A., Banks, E., Poplin, R., Garimella, K.V., Maguire, J.R., Hartl, C., Philippakis, A.A., del Angel, G., Rivas, M.A., Hanna, M., et al. (2011). A framework for variation discovery and genotyping using next-generation DNA sequencing data. Nat. Genet. *43*, 491–498.

Estrada, K., Styrkarsdottir, U., Evangelou, E., Hsu, Y.H., Duncan, E.L., Ntzani, E.E., Oei, L., Albagha, O.M., Amin, N., Kemp, J.P., et al. (2012). Genome-wide meta-analysis identifies 56 bone mineral density loci and reveals 14 loci associated with risk of fracture. Nat. Genet. *44*, 491–501.

Ferreira, R.J., Irioda, A.C., Cunha, R.C., Francisco, J.C., Guarita-Souza, L.C., Srikanth, G.V., Nityanand, S., Rosati, R., Chachques, J.C., and de Carvalho, K.A. (2012). Controversies about the chromosomal stability of cultivated mesenchymal stem cells: their clinical use is it safe? Curr. Stem Cell Res. Ther. *7*, 356–363.

Gore, A., Li, Z., Fung, H.L., Young, J.E., Agarwal, S., Antosiewicz-Bourget, J., Canto, I., Giorgetti, A., Israel, M.A., Kiskinis, E., et al. (2011). Somatic coding mutations in human induced pluripotent stem cells. Nature *471*, 63–67.

Hindson, B.J., Ness, K.D., Masquelier, D.A., Belgrader, P., Heredia, N.J., Makarewicz, A.J., Bright, I.J., Lucero, M.Y., Hiddessen, A.L., Legler, T.C., et al. (2011). High-throughput droplet digital PCR system for absolute quantitation of DNA copy number. Anal. Chem. *83*, 8604–8610.

Hussein, S.M., Batada, N.N., Vuoristo, S., Ching, R.W., Autio, R., Närvä, E., Ng, S., Sourour, M., Hämäläinen, R., Olsson, C., et al. (2011). Copy number variation and selection during reprogramming to pluripotency. Nature *471*, 58–62.

Li, H., and Durbin, R. (2009). Fast and accurate short read alignment with Burrows-Wheeler transform. Bioinformatics *25*, 1754–1760.

Li, H., Handsaker, B., Wysoker, A., Fennell, T., Ruan, J., Homer, N., Marth, G., Abecasis, G., and Durbin, R.; 1000 Genome Project Data

Processing Subgroup (2009). The Sequence Alignment/Map format and SAMtools. Bioinformatics 25, 2078–2079.

Mak, A.B., Ni, Z., Hewel, J.A., Chen, G.I., Zhong, G., Karamboulas, K., Blakely, K., Smiley, S., Marcon, E., Roudeva, D., et al. (2010). A lentiviral functional proteomics approach identifies chromatin remodeling complexes important for the induction of pluripotency. Mol. Cell. Proteomics 9, 811–823.

Park, S., Koh, Y., and Yoon, S.S. (2013). Effects of somatic mutations are associated with SNP in the progression of individual acute myeloid leukemia patient: the two-hit theory explains inherited predisposition to pathogenesis. Genomics Inform 11, 34–37.

Prockop, D.J. (1997). Marrow stromal cells as stem cells for nonhematopoietic tissues. Science 276, 71–74.

Prockop, D.J., and Keating, A. (2012). Relearning the lessons of genomic stability of human cells during expansion in culture: implications for clinical research. Stem Cells 30, 1051–1052.

Ruiz, S., Gore, A., Li, Z., Panopoulos, A.D., Montserrat, N., Fung, H.L., Giorgetti, A., Bilic, J., Batchelder, E.M., Zaehres, H., et al. (2013). Analysis of protein-coding mutations in hiPSCs and their possible role during somatic cell reprogramming. Nat. Commun. 4, 1382.

Sakamoto, K., Tamamura, Y., Katsube, K., and Yamaguchi, A. (2008). Zfp64 participates in Notch signaling and regulates differentiation in mesenchymal cells. J. Cell Sci. 121, 1613–1623.

Salem, H.K., and Thiemermann, C. (2010). Mesenchymal stromal cells: current understanding and clinical status. Stem Cells 28, 585–596.

Sensebé, L., Tarte, K., Galipeau, J., Krampera, M., Martin, I., Phinney, D.G., and Shi, Y.; MSC Committee of the International Society for Cellular Therapy (2012). Limited acquisition of chromosomal aberrations in human adult mesenchymal stromal cells. Cell Stem Cell 10, 9–10, author reply 10–11.

Sjöblom, T., Jones, S., Wood, L.D., Parsons, D.W., Lin, J., Barber, T.D., Mandelker, D., Leary, R.J., Ptak, J., Silliman, N., et al. (2006). The consensus coding sequences of human breast and colorectal cancers. Science 314, 268–274.

Wang, S., Qu, X., and Zhao, R.C. (2012). Clinical applications of mesenchymal stem cells. J. Hematol. Oncol. 5, 19.

Wang, Y., Zhang, Z., Chi, Y., Zhang, Q., Xu, F., Yang, Z., Meng, L., Yang, S., Yan, S., Mao, A., et al. (2013). Long-term cultured mesenchymal stem cells frequently develop genomic mutations but do not undergo malignant transformation. Cell Death Dis. 4, e950.

Yan, Z., Wang, Z., Sharova, L., Sharov, A.A., Ling, C., Piao, Y., Aiba, K., Matoba, R., Wang, W., and Ko, M.S. (2008). BAF250B-associated SWI/SNF chromatin-remodeling complex is required to maintain undifferentiated mouse embryonic stem cells. Stem Cells 26, 1155–1165.

Young, M.A., Larson, D.E., Sun, C.W., George, D.R., Ding, L., Miller, C.A., Lin, L., Pawlik, K.M., Chen, K., Fan, X., et al. (2012). Background mutations in parental cells account for most of the genetic heterogeneity of induced pluripotent stem cells. Cell Stem Cell 10, 570–582.

Zou, C., Chou, B.K., Dowey, S.N., Tsang, K., Huang, X., Liu, C.F., Smith, C., Yen, J., Mali, P., Zhang, Y.A., et al. (2012). Efficient derivation and genetic modifications of human pluripotent stem cells on engineered human feeder cell lines. Stem Cells Dev. 21, 2298–2311.